

# Combustion of binary system based on a double-base model propellant with HMX

Ye Z. Htwe<sup>\*†</sup> and Anatoli P. Denisjuk<sup>\*</sup>

<sup>\*</sup>D. Mendeleev University of Chemical Technology of Russia,  
125047 Moscow, Miusskaya sq., 9, RUSSIAN FEDERATION.  
Phone: +7-495-948-5317

<sup>†</sup>Corresponding author: yezawhtwe@mail.ru

Received: November 12, 2014 Accepted: April 7, 2015

## Abstract

In this work, the combustion regularities of a high energetic double-base model propellant, based on nitrocellulose (NC) and nitroglycerin (NGC), with HMX were studied by examining combustion rate and temperature distribution parameters in combustion wave at pressure range 1–10 MPa. It was found that the influence of HMX mass content (particle size  $> 20 \mu\text{m}$ ) on combustion rate of base propellant has extreme nature with the lowest value at ~50% HMX content. It was established that during the combustion process of propellant sample with 50% HMX, intensive decomposition of NC and NGC takes place in the condense phase at temperature 50–70 K lower than the inflection temperature, obtained from the temperature distribution measurements, and the resulting intermediate combustion product gases make the dispersion of thermally stable molten HMX layer into gaseous zone. The higher heat effect due to more intensive chemical reactions was also observed in the first flame zone just above the combustion surface. Based on the experimental results, the condense phase combustion mechanism was proposed.

**Keywords** : double-base propellant, HMX, combustion, temperature distribution

## 1. Introduction

Combustion regularities of propellants with cyclotetramethylene tetranitramine (HMX) were studied decades of years<sup>(1)–(6)</sup>. In the previous work<sup>(5)</sup>, based on the experimental combustion regularity results of various systems, comprising various kinds of active binders and HMX, it was established that depending on the combustion rate relation of an active binder and HMX, its mass content and particle size, the combustion process of resulting propellant may take place either as unique system, or as geometric (relay) model, or along the fast-burning binder layer. Thus, the addition of HMX may increase, decrease or not affect the combustion rate of base propellant.

However, temperature distribution measurements were not made in the above cited work<sup>(5)</sup>. Such kinds of studies were carried out by A.A. Zenin and co-authors<sup>(4)</sup> on propellant samples with 10, 15 and 30% of HMX (added above 100% of base propellant). Addition of HMX caused the fall in combustion rate of base propellant and authors concluded that the vital parameters (mainly the

combustion surface temperature ( $T_s$ ) and the temperature gradient on combustion surface ( $\phi$ ) for combustion mechanism decreased and the rise in reaction intensity was observed only at high-temperature flame zone, that doesn't have an effect on the combustion rate. It should be noted that the experimental samples in above work contain relatively small amounts of HMX, so its effect also couldn't be significant.

The combustion regularities of mixtures of HMX with high and low energetic binders (polymer+various plasticizers) were studied by V.P. Sinditskii and co-authors<sup>(6)</sup> and it was concluded that combustion of the sample with HMX takes place mainly in the gaseous zone as the experimental  $T_s$  value is the same as the evaporation temperature ( $T_{ev}$ ) of the plasticizer. HMX simply vaporizes and doesn't have enough time to decompose even in the first flame zone of nitrate ester binder.

Based on the listed above variety of opinions upon the role of HMX in the combustion process of energetic materials, it is obvious that further investigations should

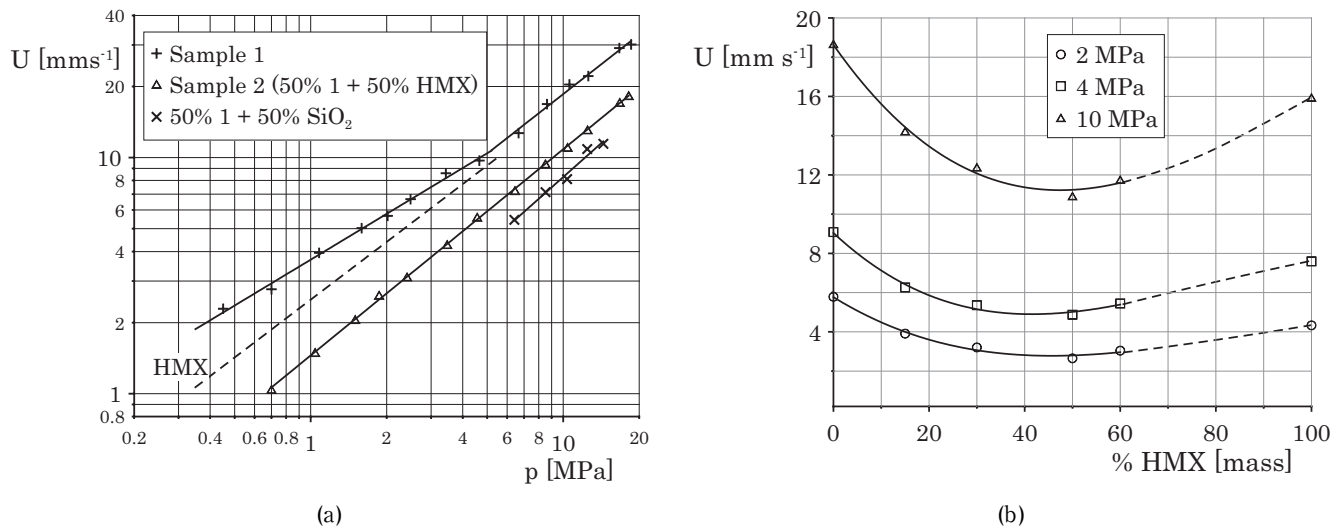


**Figure 1** (a) Influence of 50% HMX on combustion rate of high energetic double-base propellant (dotted line - combustion rate of HMX<sup>7</sup>), (b) Effect of HMX mass content on combustion rate of base propellant at various pressures.

be made in this direction.

## 2. Experimental and discussion

In the present work, the combustion regularities of a high energetic double-base model propellant (sample 1), based on nitrocellulose (NC) and nitroglycerin (NGC), with HMX (particle size  $> 20 \mu\text{m}$ ) were studied. The base propellant is superior to HMX in both energetic and ballistic properties (Table 1 and Figure 1).

Combustion rate of HMX (dotted line) was taken from the work of V.P. Sinditskii and co-authors<sup>7</sup>, in which pressed cylindrical samples of 7 mm diameter and average density of  $1.76 \text{ g} \cdot \text{cm}^{-3}$  were used.

The effect of HMX mass content on combustion rate of base propellant has extreme nature, in which the lowest value was observed at  $\sim 50\%$  HMX content (sample 2). The further addition of HMX makes rise of combustion rate, which gradually approaches to that of pure HMX (Figure 1 b). The low combustion rate in the case of fast-burning binder and fine HMX particles was predicted before<sup>5</sup> due to the higher thermal stability of HMX in condense phase, which used up some parts of heat from binder's exothermic reactions for its own heat-up, but the participation of HMX's decomposition products in the heat generation processes takes place lately in the high-temperature flame zone, that doesn't have any effect on combustion rate.

For comparison, a sample of 50% base propellant and 50% sand ( $\text{SiO}_2$ ), which is totally inert in condense phase (it only takes heat for its heating up and doesn't undergo any phase changes) was tested. The combustion rate of

resulting sample is 23–28% lower than that of sample 2 (Figure 1 a). So it can be said that despite the decrease in combustion rate, HMX has certain level of positive influence on combustion process of sample 2.

Temperature distributions in the combustion wave of sample 1 ( $p=1.2\text{--}4.4 \text{ MPa}$ ) and sample 2 ( $p=1.2\text{--}10.5 \text{ MPa}$ ) were studied by the aid of Tungsten-Rhenium alloy thin micro-thermocouples (thickness  $\sim 5 \mu\text{m}$ ).

Temperature profiles obtained for sample 2 have typical form for most of the propellants. However, it was found that the inflection temperature, which normally belongs to the emergence of thermocouple's junction from condense phase to gaseous zone, obtained from the experiments for sample 2 (let's denote it  $T_{s'}$ ) is 50–70 K higher than that of sample 1 ( $T_{s,1}$ ), and close to the evaporation temperature ( $T_{ev}$ ) of HMX<sup>7</sup> (Figure 2 and 3).

Based on the temperature distribution parameters and using the kinetic parameters for thermal decomposition of NC, NGC and HMX, the degree of decomposition ( $\eta_1$ ) of these components were calculated at  $T_{s,1}$  for sample 2, whose combustion rate is  $\sim 2$  times ( $p = 4 \text{ MPa}$ ) lower than that of sample 1. Decomposition rate constants ( $K$ ) were calculated according to the rate equation  $K = K_0 \exp(-E/RT_{s,1})$  ( $K_0$  and  $E$  values for each component are presented in table 2). Reaction zone thickness ( $l_{\text{R}}$ ) was taken to be 10% of preheated zone ( $l^*$ ), obtained experimentally from temperature distribution measurements (Figure 2b).

From Table 2, it can be seen that the majority of NC and NGC already decomposed at  $T_{s,1}$ , from which 68–79% of the base propellant ( $\eta_{2,1}$ ) could undergo oxidation reactions, resulting a large amount of gaseous intermediate combustion products, which in turn cause the dispersion of thermally stable HMX into gaseous zone. This results a narrow gas-HMX premixed zone above  $T_{s,1}$ , whose temperature couldn't be higher than  $T_{ev}$  of HMX. Thereby,  $T_{s'}$  couldn't be the combustion surface temperature of sample 2, so  $T_{s,1}$  was taken as the temperature of condense phase reaction zone.

Temperature gradient ( $\phi$ ) on the combustion surface of

**Table 1** Composition and some characteristics of samples.

| Sample           | Component<br>(Composition [mass%]) | $T_{4\text{MPa}}[\text{K}]$ | $Q_{\text{zhe}}^{\#}[\text{kJ} \cdot \text{kg}^{-1}]$ |
|------------------|------------------------------------|-----------------------------|---|
| 1                | NC (39.2)+NGC (58.8)               | 3133                        | 5619  |
| 2                | 1 (50)+HMX (50)                    | 3188                        | 5605  |
| HMX <sup>7</sup> | HMX (100)                          | 3248                        | 5590  |

#  $Q_{\text{zhe}}$  – heat of explosive transformation in liquid water

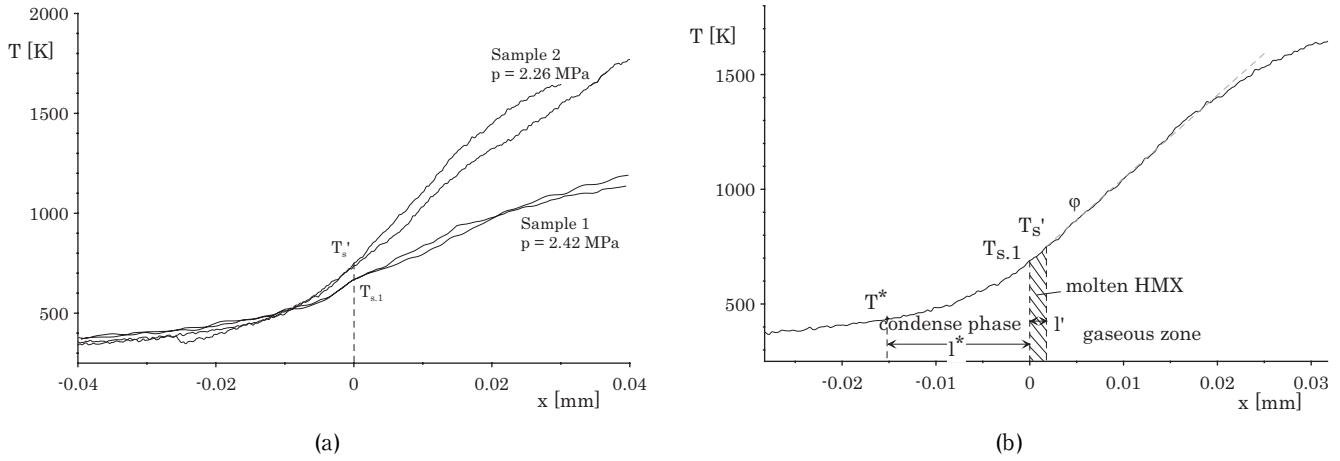


**Figure 2** (a) Temperature distributions in combustion wave of propellant samples 1 and 2, (b) Temperature distributions with proposed zone divisions near combustion surface of propellant sample 2.

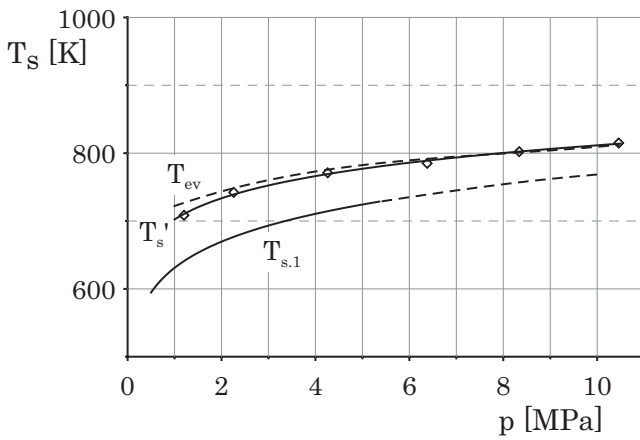


**Figure 3** Pressure dependence of condense phase reaction zone temperature and inflection temperature of sample 2 in comparison with evaporation temperature of HMX.

sample 2 is  $\sim 2$  times higher than that of propellant 1 at 4 MPa pressure and close to the results of A. Zenin and S. Finjakov<sup>8)</sup> (Figure 4). Taking into account the difference in combustion rate and density of samples ( $1.6 \text{ g} \cdot \text{cm}^{-3}$  for sample 1 and  $1.74 \text{ g} \cdot \text{cm}^{-3}$  for sample 2), influx of heat from gaseous zone to condense phase via thermal conductivity ( $q_\lambda$ ) for sample 2 is  $\sim 3.7$  times higher than that of sample 1 at 4 MPa pressure, which indicates the significant contribution of HMX in exothermic reactions just above the combustion surface (first flame zone).

Heat balance of condense phase for sample 2 was compiled as follow :

$$0.5[c_{p,1}(T_{s,1} - T_0)] + 0.5[c_{p,HMX}(T_{s,1} - T_0)] + 0.5Q_{p,c+m} + 0.5(1 - \eta_{HMX})[c_{p,HMX}(T_s' - T_{s,1})] + 0.5(1 - \eta_{HMX})Q_{ev} = q_\lambda + Q_c \quad (1)$$

in which:  $c_{p,1}$  - thermal capacity of base propellant 1 ( $1.46 \text{ J} \cdot \text{g}^{-1} \cdot \text{K}^{-1}$ );  $c_{p,HMX}$  - thermal capacity of HMX ( $= 0.3 + 2.4 \cdot 10^{-3} T \text{ J} \cdot \text{g}^{-1} \cdot \text{K}^{-1}$ );  $Q_{p,c+m}$  - heat of phase change and melting of HMX ( $33.2 \text{ J} \cdot \text{g}^{-1}$ <sup>10)</sup> and  $236 \text{ J} \cdot \text{g}^{-1}$ <sup>11)</sup> respectively);  $Q_{ev}$  - heat of evaporation of intact portion of HMX ( $423 \text{ J} \cdot \text{g}^{-1}$ <sup>7)</sup>);  $q_\lambda$  - influx of heat from gaseous zone to condense phase via thermal conductivity;  $Q_c$  - heat effect of exothermic reactions in condense phase reaction zone;  $\eta_{HMX}$  - degree of transformation of HMX, which undergoes till exothermic reactions in condense phase reaction zone. The value ( $\eta_{HMX}$ ) was assumed unknown and based on the results of heat balance equation we would determine the role of HMX in combustion mechanism of propellant sample 2.

For propellant sample 2  $Q_c$  comprises from heat effect of base propellant ( $Q_{c,1}$ ) and heat effect of HMX ( $Q_{c,HMX}$ ):

$$Q_c = Q_{c,1} + Q_{c,HMX} = 0.5Q_{NO,1}\eta_{2,1} + 0.5Q_{NO,HMX}\eta_{HMX} \quad (2)$$

where  $Q_{NO,1}$  and  $Q_{NO,HMX}$  - maximum heat effects of base propellant and HMX respectively, which could have been achieved when all the  $\text{NO}_2$  groups, contained in them,

**Table 2** Degrees of decomposition of NC, NGC and HMX at  $T_{s,1}$  for propellant sample 2.

| p [MPa] | T <sub>s,1</sub> [K] | η <sub>1</sub> [%]  |   |  | η <sub>2,1</sub> [%] of base propellant<br>lg K <sub>0</sub> =9.6 s <sup>-1</sup> .<br>E=81.6 kJ mol <sup>-1</sup> |
|---------|----------------------|---|---|--|--|
|         |                      | NC<br>lg K <sub>0</sub> =16.9 s <sup>-1</sup> .<br>E=175.8 kJ mol <sup>-1</sup> | NGC<br>lg K <sub>0</sub> =17.78 s <sup>-1</sup> .<br>E=177 kJ mol <sup>-1</sup> | HMX<br>lg K <sub>0</sub> =16 s <sup>-1</sup> .<br>E=188 kJ mol <sup>-1</sup> |  |
| 1       | 638                  | 35.8  | 93.1  | 0.6  | 68   |
| 2       | 673                  | 72.5  | 99.9  | 1.8  | 73   |
| 4       | 708                  | 94.9  | 100   | 4.6  | 74   |
| 6       | 736                  | 99.8  | 100   | 9.9  | 77   |
| 8       | 754                  | 100   | 100   | 14.9   | 78   |
| 10      | 769                  | 100   | 100   | 20.8   | 79   |

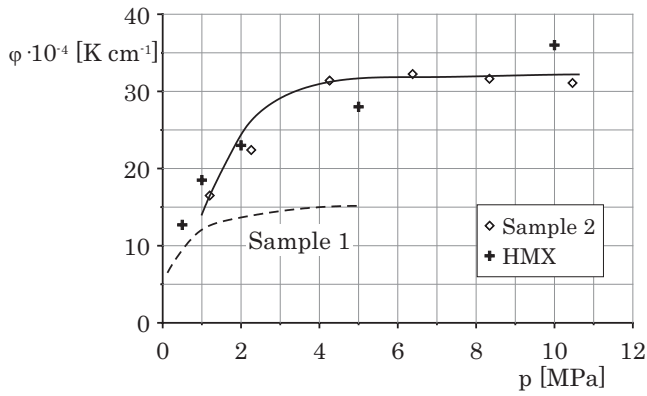


**Figure 4** Pressure dependence of temperature gradient on combustion surface of sample 2 in comparison with that of base propellant 1 and HMX<sup>8)</sup>.

transformed into NO. In pressure range 1–10 MPa,  $Q_{NO,1}$  varies in the range 1963–2039 J g<sup>-1</sup> while  $Q_{NO,HMX}$  equals to 2570–2636 J g<sup>-1</sup>. Substituting Equation 2 into Equation 1,  $\eta_{HMX}$  can be calculated as follow :

$$\eta_{HMX} = \frac{1 + 2 + 3 + 0.5[c_{p,HMX}(T'_{s,1} - T_{s,1}) + Q_{ev}] - q_{\lambda} - Q_{c,1}}{0.5[c_{p,HMX}(T'_{s,1} - T_{s,1}) + Q_{ev} + Q_{NO,HMX}]}$$

where  $1 + 2 + 3 = 0.5[c_{p,1}(T_{s,1} - T_0) + 0.5[c_{p,HMX}(T_{s,1} - T_0) + 0.5Q_{p,c+m}]]$ .

From Table 3, it can be seen that HMX doesn't take part in condense phase exothermic reactions at pressure interval 1–4 MPa ( $\eta_{HMX} = 1\%$  at 4 MPa), but heat influx from gaseous zone ( $q_{\lambda}$ ) at 1 and 2 MPa pressures is not only capable to provide necessary heat for raising temperature of HMX from  $T_{s,1}$  to  $T'_{s,1}$  (in narrow zone) and for its evaporation (4 and 5 in left hand side of heat balance equation), but also for warming up of some parts of condense phase beneath  $T_{s,1}$ . Starting from 4 MPa pressure,  $q_{\lambda}$  is consumed exclusively for evaporation of some parts of HMX. At pressure range 6–10 MPa,  $\eta_{HMX}$  in the condense phase is estimated to be 4–10%, which

accounts 7–14% of total heat effect in the condense phase reaction zone ( $Q_c$ ). In general, the majority of heat, necessary for propagation of combustion process of sample 2 at pressure range 1–10 MPa is provided by chemical reactions, occurring in the condense phase reaction zone ( $\epsilon = 51$ –86%).

The proposed mechanism of the condense phase reaction zone beneath molten HMX layer could explain the strange nature of influence of HMX content upon the combustion rate of base propellant sample 1 (the combustion rate decreases up to 50% HMX content and increases again for samples with HMX > 50%). For comparison between combustion processes of sample 2 and pure HMX, we calculated the volume of intermediate combustion products at  $T_{s,1}$  for propellant sample 2 using a simulation program REAL<sup>12)</sup>, and consequently, the rate of outflow of these gases based on the continuity of mass flow principle " $U_c \rho_c = U_g \rho_g$ ", where:  $U$  - linear velocity;  $\rho$  - density (indexes "c" and "g" correspond to condense phase and gas phase respectively).

From Table 4, it can be seen that the outflow rate of gaseous products at  $T_{s,1}$  is 84–17 times higher than the linear combustion rate. Thus, despite the same temperature values ( $T'_{s,1}$  and  $T_{ev}$ ) of sample 2 and pure HMX and slower combustion rate (~1.7 times at pressure 4 MPa), the degree of decomposition of HMX in case of sample 2 (HMX flowing together with gaseous combustion products of base propellant) could be much lower than in the combustion process of pure HMX.

In accordance with the above stated combustion mechanism for propellant sample with 50% HMX, further increase in proportion of HMX will make the decrease in volume of intermediate combustion products of NC and NGC. Hence the degree of decomposition of HMX and its heat contribution in condense phase will increase accordingly. Then the condense phase reaction zone could be shifted from  $T_{s,1}$  to a higher temperature.

**Table 3** Condense phase heat balance during the combustion process of the propellant sample 2.

| $p$ [MPa]                             | 1     | 2     | 4     | 6     | 8     | 10    |
|---------------------------------------|-------|-------|-------|-------|-------|-------|
| $U$ [cm s <sup>-1</sup> ]             | 0.145 | 0.265 | 0.484 | 0.689 | 0.885 | 1.075 |
| $T_{s,1}$ [K]                         | 638   | 673   | 708   | 736   | 754   | 769   |
| $T'_{s,1}$ [K]                        | 703   | 733   | 766   | 786   | 800   | 811   |
| $Q_{c,1}$ [J g <sup>-1</sup> ]        | 465   | 602   | 739   | 782   | 790   | 810   |
| $Q_{NO,HMX}$ [J g <sup>-1</sup> ]     | 2570  | 2584  | 2601  | 2616  | 2627  | 2636  |
| $q_{\lambda}$ [J g <sup>-1</sup> ]    | 440   | 358   | 271   | 211   | 173   | 148   |
| $1+2+3$ [J g <sup>-1</sup> ]          | 631   | 689   | 749   | 797   | 830   | 856   |
| $\eta_{HMX}$ [%]                      | 0     | 0     | 1     | 4     | 8     | 10    |
| $Q_{c,HMX}$ [J g <sup>-1</sup> ]      | 0     | 0     | 9     | 58    | 107   | 131   |
| 4 [J g <sup>-1</sup> ]                | 62    | 60    | 60    | 51    | 45    | 42    |
| 5 [J g <sup>-1</sup> ]                | 212   | 212   | 210   | 202   | 194   | 190   |
| $Q_{total}^{\#}$ [J g <sup>-1</sup> ] | 904   | 960   | 1019  | 1051  | 1070  | 1088  |
| $Q_c$ [J g <sup>-1</sup> ]            | 465   | 602   | 748   | 840   | 897   | 941   |
| $\epsilon^*$ [%]                      | 51    | 63    | 73    | 80    | 84    | 86    |
| $Q_{c,HMX}/Q_c$                       | 0     | 0     | 0.01  | 0.07  | 0.12  | 0.14  |

<sup>#</sup> $Q_{total}$  - left hand side of heat balance equation

$\epsilon^* = 100 \cdot Q_c / Q_{total}$

**Table 4** Calculation of volume and velocity of gaseous intermediate combustion products at  $T_{s,1}$  for propellant sample 2.

| $p$<br>[MPa] | $U_c$<br>[cm s <sup>-1</sup> ] | $v_g$ (100%),<br>[cm <sup>3</sup> g <sup>-1</sup> ] | $\eta_{2,1}$<br>[%] | $v_g$ (at $T_{s,1}$ ),<br>[cm <sup>3</sup> ] | $U_g$<br>[cm s <sup>-1</sup> ] | $U_g/U_c$ |
|--------------|--------------------------------|---|---------------------|--|--------------------------------|-----------|
| 1            | 0.145                          | 389   | 68                  | 52   | 12.1                           | 84        |
| 2            | 0.265                          | 199   | 73                  | 36   | 15.1                           | 57        |
| 4            | 0.484                          | 102   | 74                  | 22   | 17.4                           | 36        |
| 6            | 0.689                          | 69  | 77                  | 16   | 17.9                           | 26        |
| 8            | 0.885                          | 52  | 78                  | 13   | 17.8                           | 20        |
| 10           | 1.075                          | 42  | 79                  | 10   | 18                             | 17        |

### 3. Conclusion

1. Addition of HMX (particle size  $< 20 \mu\text{m}$ ) to a high energetic double-base model propellant causes the decrease in combustion rate. Effect of HMX mass content on combustion rate of the base propellant has extreme nature with minimum value at  $\sim 50\%$  HMX content.

2. During the combustion process of propellant sample with 50% HMX intensive decomposition of NC and NGC takes place in the condense phase at temperature 50–70 K lower than the inflection temperature, obtained from the temperature distribution measurements, and the resulting intermediate combustion product gases make the dispersion of thermally stable molten HMX layer into gaseous zone.

3. Temperature gradient on the combustion surface of propellant sample with 50% HMX is about twice higher than that of propellant alone, which indicates a significant role of HMX in exothermic reactions just above the combustion surface. At 1 and 2 MPa pressures, the heat influx from gaseous zone ( $q_i$ ) is capable of not only providing necessary heat to rise up temperature of HMX in the narrow gas-HMX premixed zone and for its evaporation, but also warming up of some parts of condense phase beneath the reaction zone.

4. Based on the results of the condense phase heat balance, it was established that at pressure interval 1–10 MPa, the condense phase reactions play the main role in the combustion process of propellant sample with 50% HMX.

### Reference

- 1) K. Sumi, N. Kubota, E. Andoh, and K. Shiromoto, Proc. 12th Int. Symp. Space Tech. Sci., Tokyo, 483–488 (1977).
- 2) N. Kubota and T. Masamoto, Proc. 16th Symp. (Int.) Combust., 1201–1209, The Combustion Institute, Pittsburgh (1977).
- 3) N. Kubota and H. Okuhara, J. Propulsion Power, 5, 406–410 (1989).
- 4) A.A. Zenin, S.V. Finyakov, V.M. Puchkov, N.G. Ibragimov and E.F. Okhrimenko, Combust., Expl., Shock Waves, 32, 276–285 (1996).
- 5) A.P. Denisyuk, V.S. Shabalin, and Yu.G. Shepelev, Combust., Expl., Shock Waves, 34, 534–542 (1998).
- 6) V.P. Sinditskii, V.Yu. Egorshchey, M.V. Berezin, V.V. Serushkin, S.A. Filatov, and A.N. Chernyi, Combust., Expl., Shock Waves, 48, 163–176 (2012).
- 7) V.P. Sinditskii, V.Yu. Egorshchey, M.V. Berezin and V.V. Serushkin, Combust., Expl., Shock Waves, 45, 461–477 (2009).
- 8) A. Zenin and S. Finjakov, Proc. 37th Int. Annu. Conf. ICT, 118: 1–18, Karlsruhe, FRG (2006).
- 9) A.A. Koptelov, Yu.M. Melohin, and Yu.N. Baranis, Proc. Conf. 75 Anni. ECTF MUCTR, 275–279 (2010) (in Russian).
- 10) P.G. Hall, Trans. Faraday Soc, 67, 556–562 (1971).
- 11) Yu.Y. Maksemov, Russ. J. phy. chem., 66, 540–542 (1992) (in Russian).
- 12) G.V. Belov, Program complex "REAL" for modeling equilibrium conditions of thermodynamic systems at elevated temperature and pressure, Bauman MSTU (2003).